KAWASAKI STEEL TECHNICAL REPORT
No.13 (September 1985)

Hydrogen Attack in Cr-Mo Steels and Disbonding or Austenitic Stainless Weld Overlay

Takuichi Imanaka, Jun-ichi Shimomura, Shozaburo Nakano, Koichi Yasuda

Synopsis :
The characteristics of a hydrogen attach on 2 1/4 Cr-1 Mo steel were studied. Resistance to the hydrogen attack increases drastically with a slight increment of increment of chromium content of around 2.25 wt%. Addition of vanadium up to 0.15 wt% and lowering silicon content to a level less than 0.15 wt% in 2 1/4 Cr-1 Mo steels improve dramatically the resistance to hydrogen attack. These improvements in the hydrogen attack can be interpreted tentatively in terms of variation in the chemistry and thermodynamically properties of carbides. Susceptibility to disbanding is generally improved by a decrease in silicon content and an increase in δ-ferrite of weld metal.

The body can be viewed from the next page.

Hydrogen Attack in Cr-Mo Steels and Disbonding of Austenitic Stainless Weld Overlay*

Takuichi Imanaka
Dr. Engi., Senior Researcher, Mizushima Research Dept., I & S Research Labs.

Jun-ichi Shimomura
Senior Researcher, Mizushima Research Dept., I & S Research Labs.

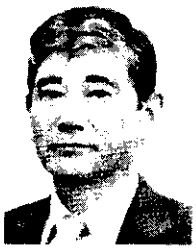

Shozaburo Nakano
Senior Researcher, Welding Lab., I & S Research Labs.

Koichi Yasuda
Senior Researcher, Welding Lab., I & S Research Labs.

Synopsis:

The characteristics of a hydrogen attack on $2\frac{1}{4}$ Cr-1 Mo steels were studied. Resistance to the hydrogen attack increases drastically with a slight increment of chromium content of around 2.25 wt%. Addition of vanadium up to 0.15 wt% and lowering silicon content to a level less than 0.15 wt% in $2\frac{1}{4}$ Cr-1 Mo steels improve dramatically the resistance to hydrogen attack. These improvements in the hydrogen attack can be interpreted tentatively in terms of variation in the chemistry and thermodynamical properties of carbides. Susceptibility to disbonding is generally improved by a decrease in silicon content and an increase in δ-ferrite of weld metal.

1 Introdiction

Various phenomena of in-service embrittlement of materials for pressure vessels, including temper embrittlement, have long been studied. Above all, hydrogen attack and the disbonding of an austenitic stainless weld overlay are currently matters of primary concern to persons interested in materials for equipment used in the chemical industry, because complete measures to prevent these have not yet been established.

Chemical equipmemt for hydrogen treatment is usually operated at temperatures between 200 and 600°C and at partial pressures of hydrogen between 10 and 600 kgf/cm^2. Carbon steels and low-alloy steels exposed to these conditions are susceptible to attack by hydrogen and show marked decreases in ductility at ambient temperature. This phenomenon of hydrogen attack is characterized by the fact that ductility, toughness and strength all decrease abruptly after an incubation period peculiar to each material. This is considered to occur because the hydrogen which has penetrated into steel reacts with carbides to nucleate methane bubbles along the grain boundary and these methane bubbles grow and ultimately link up to form fissures.

To assure corrosion resistance, austenitic stainless steel is often overlay-welded on the inside of pressure vessels. Disbonding is sometimes observed near the interface between base metal and weld metal after such pressure vessels were operated at high temperatures and in a high pressure hydrogen atmosphere. In recent years, therefore, the reexamination of overlay welding techniques has been a matter of concern. It is considered that disbonding is induced by hydrogen which, during operation, is occluded into the wall of the pressure vessel from the austenitic stainless weld overlay on the inner wall and accumulates abnormally at the interface between base metal and weld metal during a shutdown.

Remarkable progress has been made in reducing impurity elements in recent converter refining processes such as hot-metal pretreatment, ladle refining, and vacuum treatment. For example, the contents of Sb, Sn,

* Originally published in *Kawasaki Steel Giho* 17(1985)1, pp. 84-92

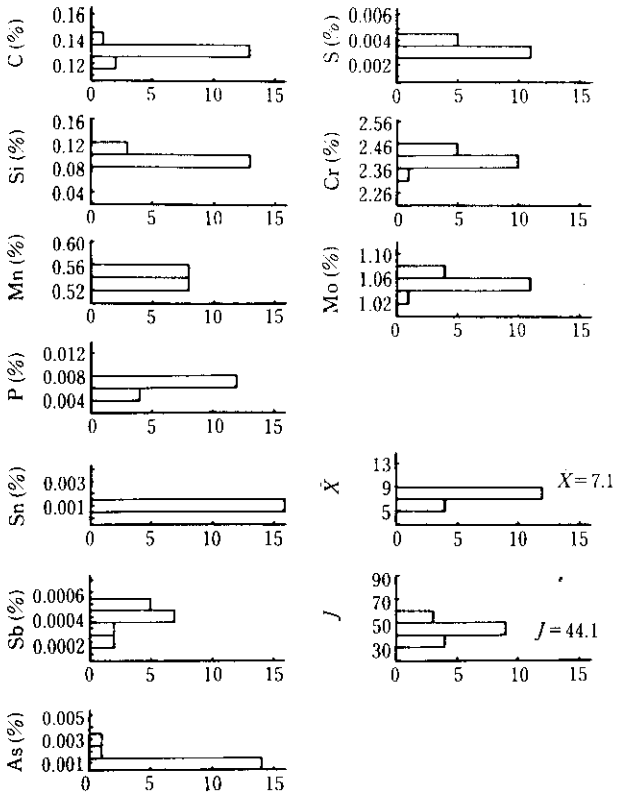

Fig. 1 Histograms of element contained in $2\frac{1}{4}$Cr-1Mo steels produced in Mizushima Works

and As, which have to date posed problems as they increase susceptibility to temper embrittlement, have been reduced to the order of ppm or trace. In another words, these contents have been sufficiently reduced at a level of less than 10 ppm, and less than 50 % of what is called the $\bar{X}$*1 and J factors.*2 **Figure 1** shows histograms of these elements of converter-refined $2\frac{1}{4}$Cr-1Mo steels produced recently at Mizushima Works (with heats as abscissa). As is apparent from this figure, it is quite unnecessary to take into consideration temper embrittlement by these impurity elements. With respect to temper embrittlement, it is necessary to consider only Si and P, especially when the cooperative effects of the two may exist.[1,2]

The cooperative effect of Si and P on temper embrittlement characteristics is shown in **Fig. 2**. Changes in the ductile-brittle transition temperature due to accelerated embrittling treatment (GE type step cooling) are plotted as a function of the P content. This figure shows that susceptibility to temper embrittlement due to P increases with increasing Si content and that temper embrittlement does not occur at all if P content is

*1 $\bar{X} = (10P + 4Sn + 5Sb + As) \times 10^{-2}$(ppm)
*2 $J = (Si + Mn)(P + Sn) \times 10^{4}$(%)

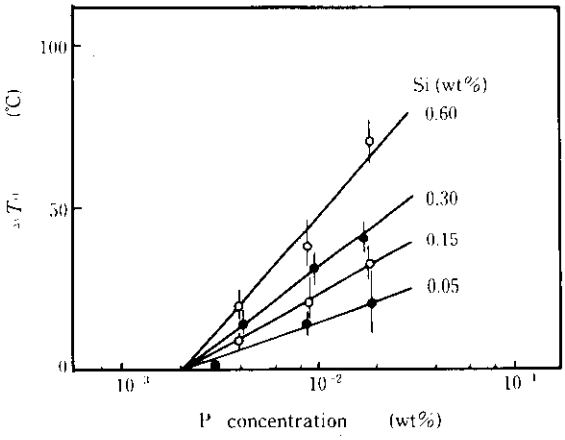

Fig. 2 Effect of P content on the transition temperature changes as a function of Si content

reduced to 0.002 wt% or less, when Si content is less than 0.6 wt%. With present steelmaking techniques, it is not difficult to maintain P content at this level. Thus, it may positively be said that the temper embrittlement of Cr-Mo steels can now be completely suppressed by controlling P and Si contents through application of recent advances in refining techniques.

Partly because the technology related to pressure vessels used in high-temperature and high-pressure hydrogen atmospheres, such as direct desulfurization reactors, is relatively new, quite unforeseen phenomena are often experienced with respect to hydrogen attack and disbonding. The explosion accident[3] at the Kashima Refinery in 1982 is an example of this. The Nelson diagram[4] that specifies the service limit of pressure vessel steels in high-temperature and high-pressure hydrogen atmospheres is proposed based on actual experiance with equipment failure and the results of operation. Metallurgical factors, such as effects of impurity elements, microstructure, and heat treatment, are not taken into consideration in this diagram, as its physical basis is at present not clarified.

The objective of the present paper is to review the interesting findings concerning the hydrogen attack and disbonding recently obtained in Research Laboratories.

2 Hydrogen Attack in Cr-Mo Steels

2.1 Changes in Mechanical Properties

2.1.1 Effect of chromium[5]

It is well known that the carbide formers elements such as Cr, Mo, W, V, Ti, Zr and Nb, improve resistance to hydrogen attack.[6] This effect increases in order as the elements are here listed, and is especially marked in such strong carbide formers as Nb, Zr, V and Ti.

Figure 3 shows changes in absorbed energy at 0°C as a function of exposure time in a case where Cr-Mo steels

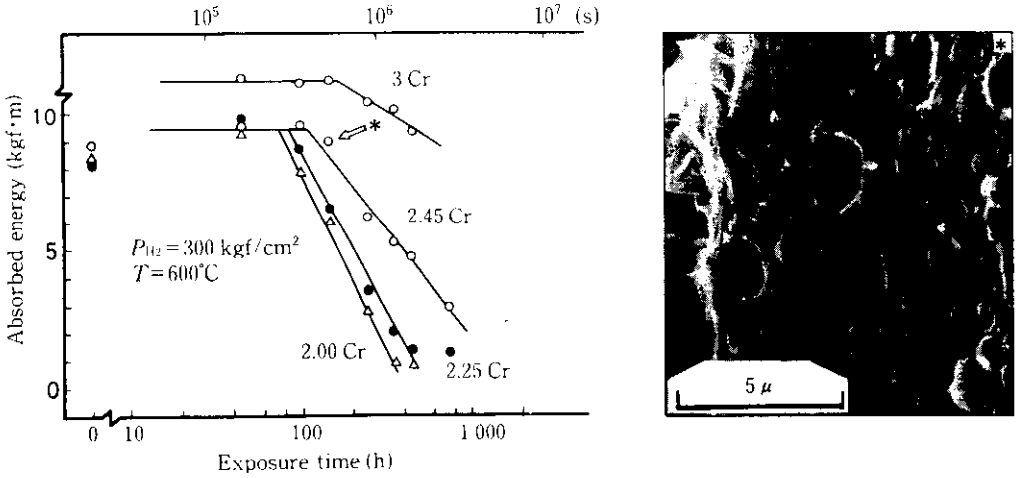

Fig. 3 Changes in absorbed energy during high temperature and high pressure hydrogen atmosphere, showing the effect of chromium content on the deterioration of toughness

with 1 wt% Mo and Cr contents of 2.00, 2.25, 2.45 and 3.15 wt% were exposed to a hydrogen atmosphere at a pressure of 300 kgf/cm^2 and a temperature of 600°C. The decrease in absorbed energy due to exposure is suppressed with increasing Cr contents of 2.00 wt% or over. This tendency is especially strong at Cr contents of 2.45% or more. The scanning electron micrograph in the figure shows the result of observation of the fractured surface area marked with an arrow. It can be seen that intergranular fracture occurred partially when absorbed energy decreased. Traces of bubbles can be observed at the grain boundary.

2.1.2 Effect of vanadium addition[7]

A hydrogen attack test was conducted on 2¼Cr-1Mo steels with V contents between 0 and 0.25 wt% at 600°C at a pressure of 450 kgf/cm^2. Results of the test are shown in **Fig. 4**. No effect of vanadium addition is observed at V contents of 0.1 wt% or below. It is apparent, however, that resistance to hydrogen attack is improved by adding vandium in amounts of 0.17 wt% or more.

2.1.3 Effect of silicon[6, 7, 8]

The Charpy impact test was performed at 0°C on 2¼Cr-1Mo steels with Si contents between 0.05 and 0.60 wt%, which had been subjected to hydrogen pressure of 300 kgf/cm^2 at 600°C. **Figure 5** represents the changes in crystallinity as a function of exposure time. The time to the appearance of intergranular fracture depends on Si content; the higher the Si content, the sooner the appearance of intergranular fracturing. A scanning electron micrograph of a fractured surface is shown also in the figure. Traces of methane bubbles are observed on the grain surfaces. All of the specimens annealed at 600°C in an Ar atmosphere fractured in the

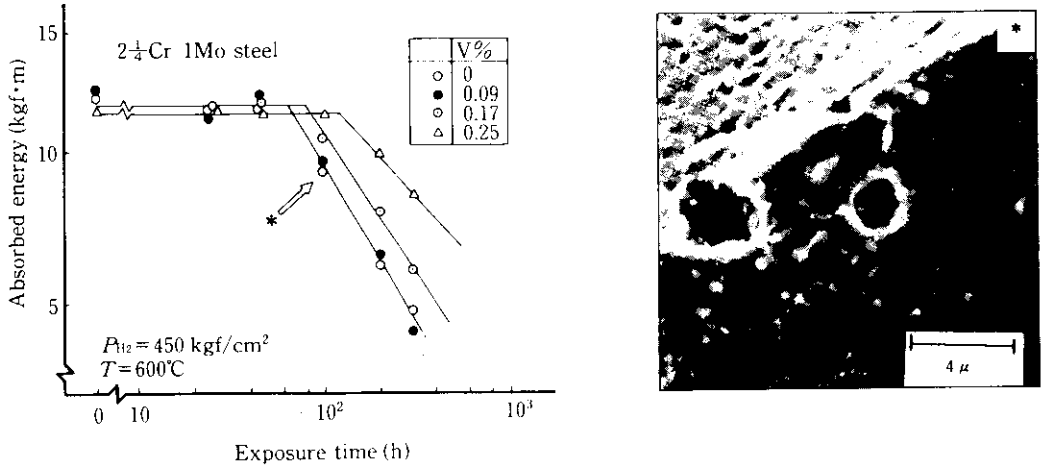

Fig. 4 Effect of vanadium addition to 2¼Cr-1Mo steels on hydrogen attack

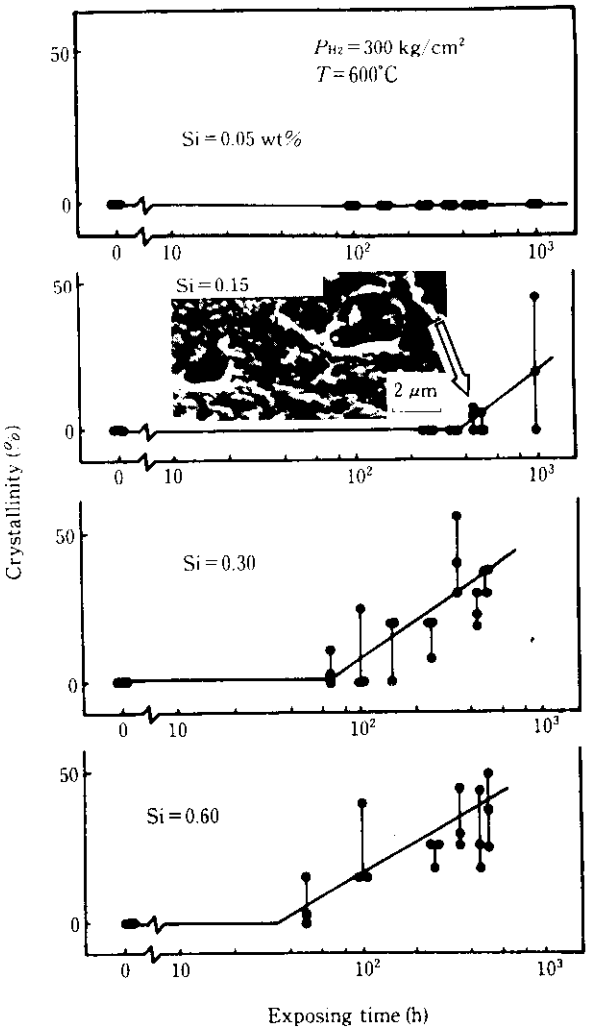

Fig. 5 Effect of silicon content in 2¼Cr-1Mo steels on crystallinity obtained by impact tests at 0°C

ductile mode.

2.2 Shape of Carbides[1, 2, 5]

Precipitates in the tempered 2 to 2.45Cr-1Mo steels were extracted by the carbon extraction replica method, and a quantitative analysis of precipitates on the grain boundary was conducted by STEM-EDS (Scanning transmission electron microscopy-Energy dispersive spectroscopy). Results of this analysis are shown in **Fig. 6**. The numerical figures in Fig. 6 denote the population of the specified carbides. The precipitates are all alloy carbides containing Fe, Cr and Mo. Dependig on composition of the specimens, the carbides on the grain boundary are divided into two classes: Cr-rich $(Fe_{45}Cr_{55})_xC_y$- type carbides and Fe-rich carbides. Fe-rich carbides change in composition from $(Fe_{0.55}Cr_{0.45})_xC_y$ to $(Fe_{0.7}Cr_{0.3})_xC_y$as the Cr content decreases from 2.45 to 2.00 wt%. These Fe-rich carbides, as shown by arrows in **Photo 1**, are coarse and granular. These coarse carbides are much observed in 2Cr-1Mo steel. As a result of electron diffraction, the crystal structure of these carbides was found to be of the M_3C-type. When extraction residues of the precipitates were subjected to X-ray diffraction, it was found that the intensity of the X-rays diffracted from M_3C-type precipitates depends very strongly on the Cr content, and that the lower the Cr content, the more frequently M_3C-type carbides will appear. These results suggest that in 2 to 2.45 Cr-1 Mo steels, susceptibility to hydrogen attack is governed by the existence of M_3C-type carbides and their chemical properties.

Carbides in tempered 2¼Cr-1Mo steels with different Si contents can be classified into three types:

Type I: $(Fe_5, Cr_{45-20}, Mo_{50-75})_x\ C_y$

Type II: $(Fe_{40}Cr_{55}Mo_5)_xC_y$

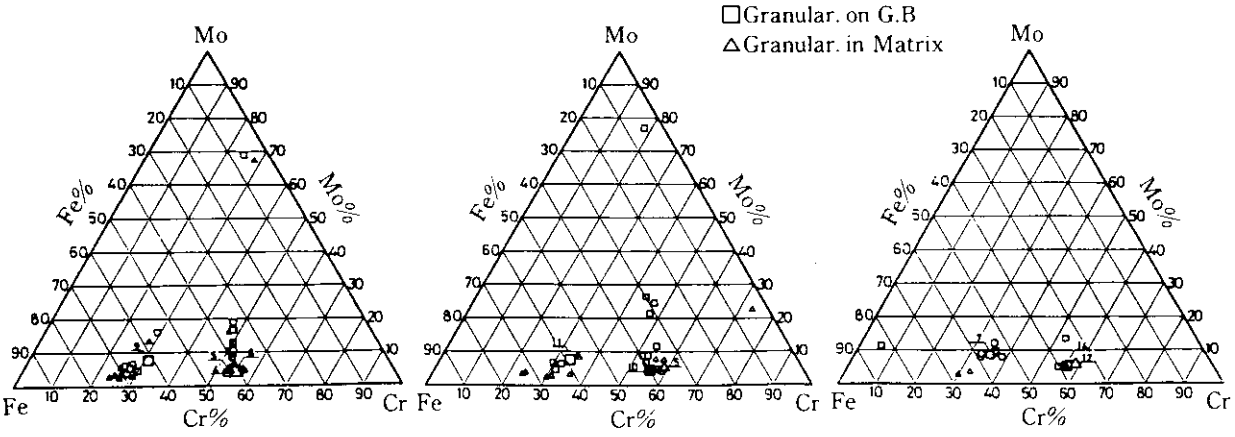

(a) Norm-Temp. Cr = 2.00 (wt%)

(b) Norm-Temp. Cr = 2.25 (wt%)

(c) Norm Temp. Cr = 2.45 (wt%)

Fig. 6 Results of STEM-EDS X-ray analyses of carbides, showing the variation in composition of carbides in accordance with chromium contents

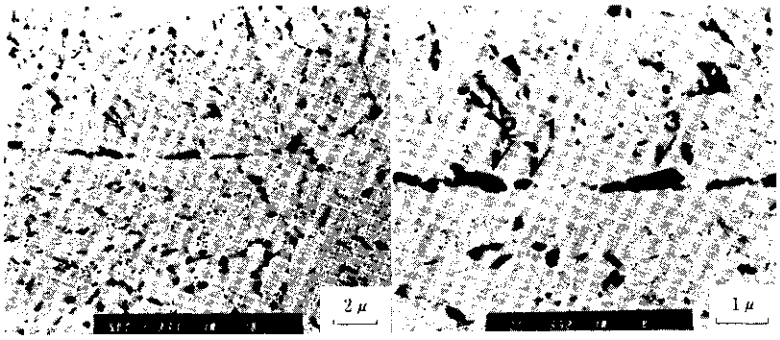

(a) Carbon extraction replica of carbids

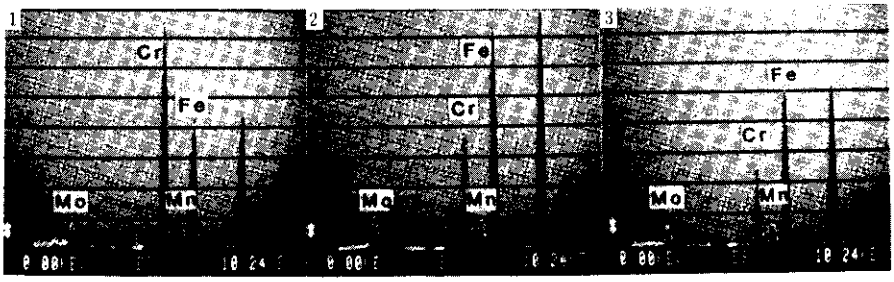

(b) EDS

Photo 1 Morphology and STEM-EDS X-ray analyses of carbides in 2.0Cr-1Mo steel

Type III: $(Fe_{55}Cr_{35}Mo_{10})_xC_y$[1].

Carbides of type I are needle-like precipitates in the grain interior with an M_2C-type crystal structure. Carbides of type II and type III are granular or plate-like precipitates. Carbides of type II frequently form in low-Si steels, and those of type III increase with increasing Si content. Furthermore, many carbides of type II have an M_7C_3-type crystal structure, while many carbides of type III have an $M_{23}C_6$ crystal structure. Similar results were also obtained by Pilling and Rindley.[9] What is interesting here is the fact that the composition of precipitates does not change continuously from type II to type III, as is apparent from Fig. 6, and that these types have definite respective compositions.

2.3 Kinetics of Hydrogen Attack[1, 8]

If incubation time t_i for hydrogen attack is defined as the time before the start of a decrease in absorbed energy following exposure of a steel to a high-temperature, high-pressure hydrogen atmosphere, then it may be considered a function of temperature and hydrogen pressure. This t_i is inversely proportional to the nth power of the pressure of hydrogen and can be formulated as a thermal activation process with apparent activation energy Q as shown in the following equation:

$$t_i = C \cdot P_{H_2}^{-n} \exp(Q/RT), \cdots\cdots\cdots\cdots (1)$$

where P_{H_2} is the partial pressure of hydrogen (kgf/cm^2) and T is the absolute temperature (K). Then, $n = 3$ and $Q = 32\,000$ cal/mol for $2\frac{1}{4}$Cr-1Mo with different Si contents. Since C is a constant, it varies with Si content. $C = 1.1 \times 10^2 h \cdot kg^{-3} \cdot cm^{2/3}$ for 0.05 to 0.15 wt% Si and $C = 2.4 \times 10\ h \cdot kg^{-3} \cdot cm^{2/3}$ for 0.30 to 0.60 wt% Si. It is apparent from these results that hydrogen attack will begin in about ten years in a hydrodesulfurization plant of conventional steel containing about 0.3% Si, when the plant is operated at a hydrogen pressure of 150 kgf/cm^2 and a temperature of 455°C. The material deterioration resulting from hydrogen attack will begin in 20 years, however, in a plant made of a well selected low-Si steel.

3 Features of Disbonding Observed in Weld Overlay

3.1 Structure and Disbonding in the Transition Zone of Overlay Weld

Photo 2 shows the microstructure and disbonding observed in the transition zone between the type 308 stainless steel overlay weld metal and the base metal of $2\frac{1}{4}$Cr-1Mo steel. A carbide precipitation layer formed during post weld heat treatment (690°C, 30 h) exists along a fusion line in the transition zone between the base metal and the weld metal. In many cases, coarse austenite grains are formed in the weld metal side of the carbide precipitation layer. Carbides precipitated during post weld heat treatment are observed at the grain boundary. Cracks can be seen to have propagated along the coarse grain boundary. As indicated by the arrows a,

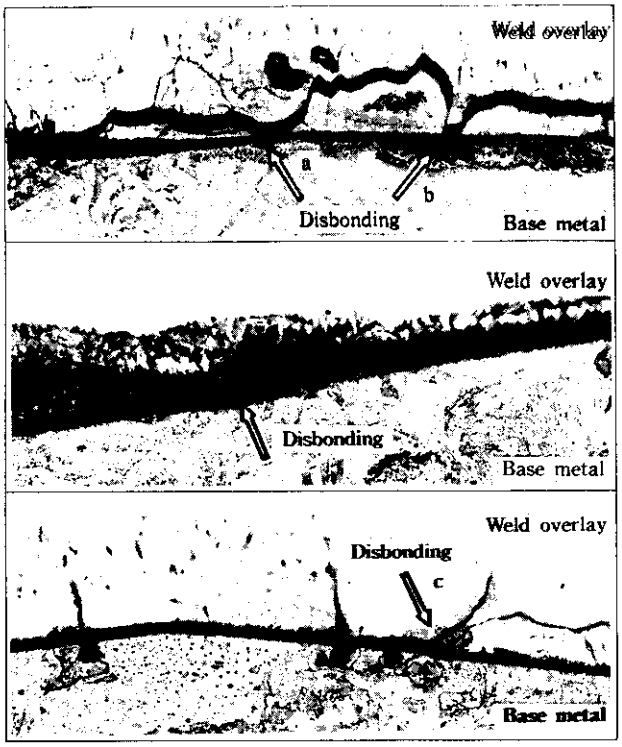

Photo 2 Microstructure and disbonding observed in the transition zone between overlay weld metal of type 308 stainless steel and base metal of $2\frac{1}{4}$Cr-1Mo steel

b and c in the photo, disbonding often seems to be initiated from a carbide precipitation layer.

3.2 Diffusion Behavior of Hydrogen near the Transition Zone of Overlay Weld[10]

During the steady-state operation of a reactor, hydrogen penetrates into the overlay weld surface, which is the inner surface of the vessel, and diffuses to the outer side of the vessel through the vessel wall, remaining in the steady state indicated by the straight line in **Fig. 7**. The behavior of hydrogen, however, is more complex during shutdowns.

In general, the diffusion behavior of hydrogen in steel follows Fick's first and second laws.

$$\mathbb{J} = -D\mathbb{V}c \quad \cdots\cdots (2)$$

$$\frac{\partial c}{\partial t} = -\mathbb{V}\mathbb{J} \quad \cdots\cdots (3)$$

Where $\mathbb{J}$ is the hydrogen flux, D is a diffusion constant, c is concentration, and t is time. Hydrogen diffuses in accordance with these equations in given phases, where the activity coefficient is uniform. That is to say, the concentration gradient is the driving force of the diffusion. When a transition between different phases exists, however, the two phases have different activity coefficients in the transition zone. In these cases, therefore, hydrogen diffuses with the activity gradient at the transition zone, rather than the concentration gradient, as the driving force. This is because, although activity is continuous, hydrogen concentration is discontinuous.

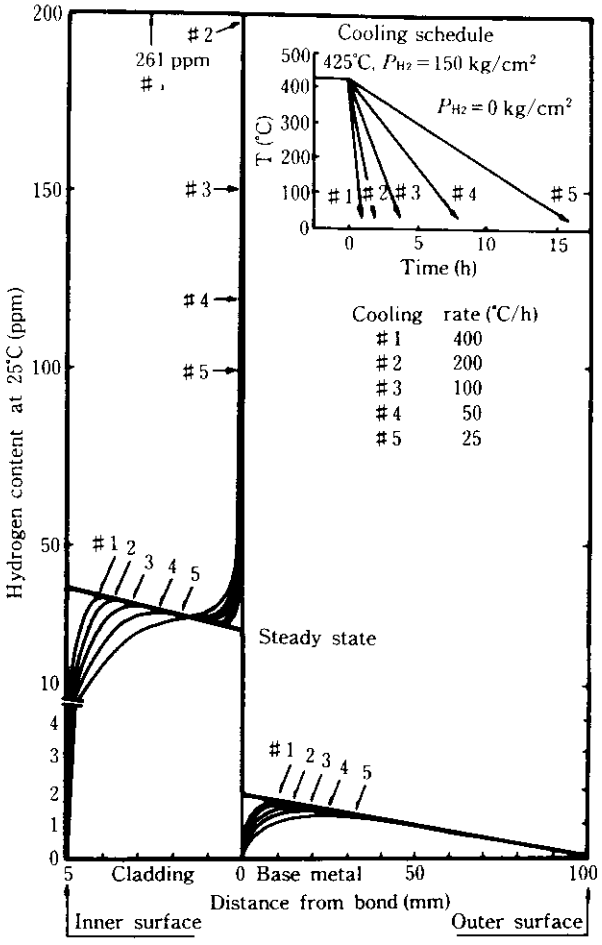

Fig. 7 Effect of cooling rates on hydrogen distribution across reactor wall at 25°C

If the two phases are the γ-phase and α-phase, the following equation holds:

$$\gamma_\gamma c_\gamma = \gamma_\alpha c_\alpha, \quad \cdots\cdots (4)$$

where

$a = \gamma c$

a: Activity

γ: Activity coefficient.

Since the hydrogen flux in the γ-phase is equal to that in the α-phase at the interface, the following equation holds:

$$D_\gamma \mathbb{V}c_\gamma = D_\alpha \mathbb{V}c_\alpha. \quad \cdots\cdots (5)$$

The hydrogen concentrations at the interface c_γ and c_α, can be calculated from Eqs. (4) and (5). Incidentally, the hydrogen concentration on the inner surface of a vessel,

c_s, is given by:

$$c_s = \sqrt{P_{H_2}} \cdot C_0 \exp(-Q/RT), \cdots\cdots\cdots (6)$$

where P_{H_2} is the partial pressure of hydrogen and C_0 and Q are constants. The hydrogen concentration distribution across the reactor wall was calculated, using appropriate constants, for a case where the reactor vessel was shut down with various cooling rates after ordinary operation (temperature, 425°C; P_{H_2}, 150 kgf/cm^2). Results of the calculation are shown in Fig. 7. Although the hydrogen distribution is in a steady state when the reactor vessel is in an ordinary operating condition, the continuity of activity of hydrogen is lost at the interface between the weld metal (austenite phase) and the base metal (ferrite phase) due to a drop in the temperature of the vessel wall during shutdown. The activity of hydrogen on the base metal side increases, with the result that the hydrogen in the vessel wall surges back in the weld metal from the base metal. Furthermore, the diffusion coefficient of hydrogen in the weld metal is smaller than that in the base metal. As a consequence, hydrogen accumulates abnormally at the weld metal side of the interface. This abnormal accumulation of hydrogen is remarkable when the cooling rate is high. It is considered that this abnormal accumulation of hydrogen contributes to the propagation of disbonding.

3.3 Chemical Composition of Weld Metal and Disonding[11, 12]

Factors affecting disbonding can be summarized as follows:[13]

(1) When coarse austenite grains exist, disbonding often propagates along the grain boundaries. In some cases, disbonding propagates in carburized zones.
(2) The initiation point of disbonding has not yet been examined. As mentioned previously, however, results of numerous investigations suggest that disbonding is initiated in a carbide precipitation layer. This carbide precipitation layer is formed during post weld heat treatment.
(3) Coarse grains are observed in an as-welded overlay metal. They are not formed during postweld heat treatment, but formed during overlay-welding.
(4) When postweld heat treatment is not conducted, disbonding does not occur, regardless of the existence of coarse grains. However, an abnormal accumulation of hydrogen takes place.
(5) Abnormal accumulation of hydrogen occurs regardless of the existence of carbide precipitation layers. That is to say, the existence of a carbide precipitation layer in the boundary is not taken into consideration in the above-mentioned calculation process.
(6) When the base metal is a low carbon steel (C < 0.01 wt%), disbonding does not take place because a carburized layer is not formed, even if postweld heat treatment is conducted.

It can be concluded from the foregoing that the main cause of disbonding is the carbide precipitation layer formed by post weld heat treatment.

Since cracks generally undergo the processes of initiation and propagation, it suffices to consider controlling initiation and propagation separately as measures to prevent disbonding. The initiation of disbonding has not been thoroughly examined to date. However, considering the fact that the initiation lacation of disbonding is in a carburized layer, the properties and the state of existence of carbides may have an effect on the initiation of disbonding. That is to say, the initiation of disbonding could possibly be controlled by adding elements that form stable carbides, such as Ti and Nb, and those affecting the activity of carbides, such as Si, Al and B, and by controlling elements that change the activity of carbon, such as Ni and Cr.

With respect to the propagation of disbonding, it is important to control the amount of δ-ferrite, which is considered effective in suppressing the formation and growth of coarse austenite grains, since such austenite grains form the propagation path for disbonding, as mentioned above. For example, in the δ-ferrite-free weld metal, the coarse austenite grains grow up to 200 μm from the weld interface. This suggests that the phase control by the balance of the Ni and Cr equivalents in the Delong-Schaeffer diagram plays an important role in suppressing the formation of the coarse austenite grains.

Based on this consideration, a disbonding test was conducted on the overlay welds with weld metals of various Si content and δ-ferrite content some of results are shown in **Fig. 8**. The δ-ferrite content, as abscissa in the figure, represents the δ-ferrite content on the austenite-martensite boundary line (A-M line) determined from measurement results on actual weld metal. It can be seen from this that the formation of coarse grains can be almost completely prevented by ensuring δ-ferrite contents on the A-M line of 5% or more.

4 Discussion

4.1 Hydrogen Attack

As mentioned earlier, hydrogen attack is a phenomenon in which hydrogen that has entered steel in a high temperatures and high pressures atmosphere generates methane bubbles by reacting with carbon precipitates in the steel, thus deteriorating the steel's ductility and toughness at room temperature. Therefore physical and chemical properties of in-steel carbides determine the resistivity of the steel. The deterioration of steel in a high-temperature, high-pressure hydrogen atmosphere

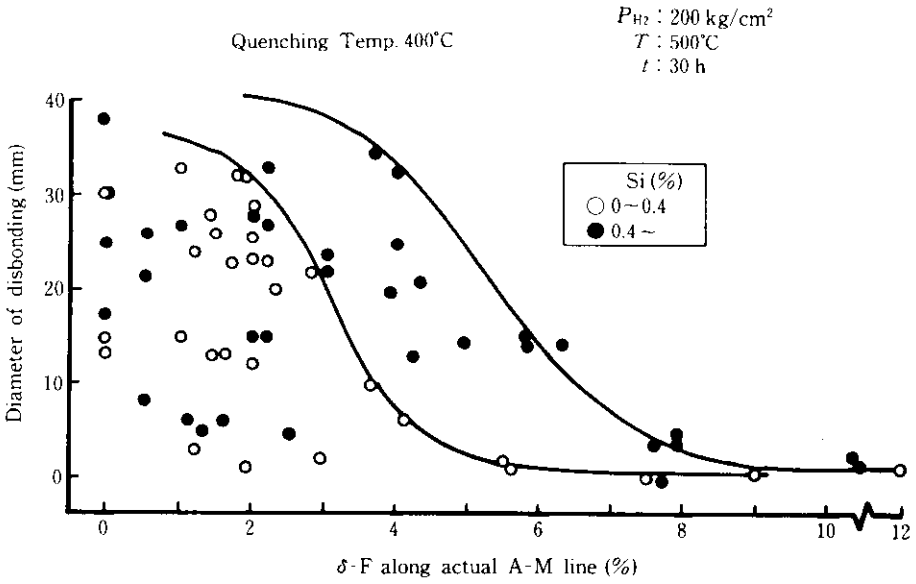

Fig. 8 Influence of silicon contents and δ-ferrite contents in weld metal upon disbonding

is essentially caused by the reaction:

$$2H_2 + C = CH_4. \cdots\cdots\cdots\cdots\cdots\cdots \textbf{[I]}$$

When this reactin occurs inside steel, methane is trapped at the phase boundaries, forming voids which eventually grow and link, developing into large cracks. As a result, the mechanical properties of the steel deteriorate. This happens when the equilibrium of the reaction is shifted to the right side in the equation above due to a sufficient partial pressure of methane. Therefore, the possibility of hydrogen attack depends on the pressure of methane. Carbon is present predominantly as carbides, so the methane reaction can be formulated as follows:

$$2H_2 + M_xC = CH_4 + xM. \cdots\cdots\cdots\cdots \textbf{[II]}$$

This reaction contains as component reactions, reaction [I] and reaction [III]:

$$xM + C = M_xC. \cdots\cdots\cdots\cdots\cdots\cdots \textbf{[III]}$$

Therefore, the change in free energy of reaction [II], ΔG^{II}, is given by the following equation using the free energy of methane formation of reaction [I], ΔG^{I}, and that of carbide formation of reaction [III], ΔG^{III}:

$$\Delta G^{II} = \Delta G^{I} - \Delta G^{III} + x\Delta\bar{G}_M, \cdots\cdots\cdots \textbf{[IV]}$$

where $\Delta\bar{G}_M$ is the partial molar free energy of metal or metals in solid solution in steel. The equilibrium constant K^{II} of reaction II is given by Eq. (7):

$$K^{II} = \frac{f_{CH_4}}{f^2_{H_2}} = \exp\left(-\Delta G^{II}/RT\right), \cdots\cdots\cdots \textbf{(7)}$$

where f_{CH_4} and f_{H_2} are the fugacity of methane and hydrogen, respectively. The above-mentioned effect of Si on the kinetics of hydrogen attack and the significant effect of a slight Cr content difference on susceptibility to hydrogen attack must be explained by a difference in K^{II} in Eq. (7).

The partial pressure of methane is decisively governed by the properties of carbides in steel. In the case of the above-mentioned 2Cr-1Mo steel and 2.45Cr-1Mo steel, for example, two types of carbides exist at the grain boundaries as shown in Fig. 6, and the effect of the Cr content of the steel is observed in precipitates of type II (Fe-rich precipitates). As a result of study by X-ray diffraction, the existence of M_3C-type carbides can be considered to be a critical factor influencing susceptibility to hydrogen attack. Therefore, reaction [II] takes the following forms:
for 2Cr-1Mo steel,

$$2H_2 + (Fe_{0.7}Cr_{0.3})_3C = CH_4 + 2.1\underline{Fe} + 0.9\underline{Cr}, \cdots\cdots \textbf{(8)}$$

for 2.45Cr-1Mo steel,

$$2H_2 + (Fe_{0.55}Cr_{0.45})_3C = CH_4 + 1.65\underline{Fe} + 13.5\underline{Cr}, \cdots\cdots \textbf{(9)}$$

where $\underline{Fe}$ and $\underline{Cr}$ represent the Fe atom and Cr atom in solution. To calculate changes in the free energy of the two reactions, it is necessary to determine the free energy of methane formation, the free energy of formation of alloy carbides, and partial molar free energies of Fe atoms and Cr stoms in solution.

The free energy of methane formation, ΔG^{I}, is given by the following equation, after Kubaschewiski and Evans:[14]

$$\Delta G^{I} = -16520 + 12.25T \log T - 15.62T \text{ cal/mol.} \quad \cdots\cdots\cdots\cdots (10)$$

The free energy of formation of alloy carbide, ΔG^{III}, is given by the following equation after Richardson:[15]

$$\Delta G^{III} = N_{Fe_3C}[\Delta G_{Fe_3C} + RT \ln (N_{Fe_3C})^3] + N_{Cr_3C}[\Delta G_{Cr_3C} + RT \ln (N_{Cr_3C})^3], \quad \cdots\cdots\cdots\cdots\cdots\cdots (11)$$

where N_{Fe_3C} and N_{Cr_3C} are molar fractions for a case where the alloy carbide M_3C is composed of Fe_3C and Cr_3C, and ΔG_{Fe_3C} and ΔG_{Cr_3C} are the free energy of formation of Fe_3C and Cr_3C. ΔG_{Fe_3C} is given by the following equation:

$$\Delta G_{Fe_3C} = 6380 - 5.92T \text{ cal/mol.} \quad \cdots\cdots\cdots (12)$$

With respect to the theoretically derived Cr_3C, the free energy of formation has been calculated by Sharma et al.[16] and is given by:

$$\Delta G_{Cr_3C} = -17416.2 + 5.07T \ln T - 43.05T \text{ cal/mol.} \quad \cdots\cdots\cdots (13)$$

When ΔG^{III} is calculated by applying the above-mentioned experimental results for carbides obtained in the present investigation and mentioned above to these equations, −9838 cal/mol for 2Cr-1Mo steel and −7114 cal/mol for 2.45Cr-1Mo steel are obtained.

If the activity of a metal M is denoted by a_M, the partial molar free energy of Fe and Cr in solution is given by:

$$\Delta \bar{G}_M = RT \ln a_M. \quad \cdots\cdots\cdots\cdots\cdots\cdots (14)$$

On the assumption that the Fe-Cr solid solution is a regular solid solution, a_{Cr} can be calculated[20] using the relationship between the Cr content of alloy and the Cr content of ferrite in equilibrium with carbides, obtained from the published data on Fe-Cr-C alloys by Ku[17] and Jellinghaus and Keller.[18] We obtain −5109 cal/mol and −4661 cal/mol as $\Delta \bar{G}_{Cr}$ at 600°C for 2Cr-1Mo steel and 2.45Cr-1Mo steel, respectively. With respect to $\Delta \bar{G}_{Fe}$, the activity of an Fe atom is equal to its molar fraction if an Fe atom in ferrite is supposed to follows Raoult's law. $\Delta \bar{G}_{Fe}$ at 600°C is −13.9 cal/mol for 2Cr-1Mo and −19.2 cal/mol for 2.45Cr-1Mo steel. From these values, ΔG^{II} and K^{II} at 600°C are as follows:

for 2Cr-1Mo steel,

$$\Delta G^{II} = 6507 \text{ cal/mol},$$
$$K^{II} = 2.4 \times 10^{-2},$$

for 2.45Cr-1Mo steel,

$$\Delta G^{II} = 9148 \text{ cal/mol},$$
$$K^{II} = 5.1 \times 10^{-3}.$$

From Eq. (7),

$$f_{CH_4} = K^{II} \cdot f_{H_2}^2 = K^{II} \cdot P_{H_2}^2.$$

Hence, f_{CH_4} is 211 kgf/cm² for 2Cr-1Mo steel and 45 kgf/cm² for 2.45Cr-1Mo steel. Incidentally, it may be thought that $f_{CH_4} \cong P_{CH_4}$ when fugacity takes values on this order. For the methane bubble to grow, the condition that $P_{CH_4} > 2\gamma/r$ must be satisfied, where r is the radius of the methane bubble and γ is its surface tension. If $\gamma \cong 10^{-3}$ kgf/cm² and $r \simeq 1$ to 2 μm, then $P_{CH_4} > 10^3$ kgf/cm². Thus, the value obtained above is lower by about one order of magnitude. However, the above calculation applies to a case where ferrite is in equilibrium with carbides, and it should be condisered that they are in an unstable non-equilibrium state. In this case, K^{II} takes high values and there is some uncertainty in thermodynamical parameters, especially the formation energy of the theoretical carbide that exists only theoretically, Cr_3C. In view of these factors, it may be thought that the obtained results sufficiently explain the difference in susceptibility to hydrogen attack between 2Cr-1Mo steel and 2.45Cr-1Mo steel.

The effect of Si might be considered as follows. As described in Sec. 2.2, many carbides on the grain boundaries of low-Si steels are Cr-rich Fe-Cr-Mo alloy carbides of type II and many carbides in high-Si steels are Fe-rich alloy carbides of type III. Many carbides of type II have an M_7C_3-type crystal structure and many carbides of type III have an $M_{23}C_6$-type crystal structure. According to Geiger and Angeles,[20] the equilibrium constant of reaction II (see Sec. 4.1) of Cr_7C_3 is smaller than that of $Cr_{23}C_6$ in tempered $2\frac{1}{2}$Cr-1Mo steels. The effect of Si on hydrogen attack can be explained based on these facts and the finding, obtained in the present investigation, that K^{II} increases with increasing Fe content in Fe-Cr alloy carbides. To evaluate the difference in susceptibility to hydrogen attack among various steels more quantitatively, however, it is necessary to determine accurately the activity of carbon atoms for each steel grade.

4.2 δ-Ferrite in Weld Metal[11, 12]

As shown in **Fig. 9**, when the transition of the composition from base metal ($2\frac{1}{4}$Cr-1Mo steel) to weld metal (with various compositions) is approximated by a straight line in the Delong-Schaeffler diagram, it is found that weld metal contains less austenite in the constituent phase as the composition of the weld metal changes from Depo ① to Depo ③. This means that the formation of coarse austenite grains can be prevented by properly controlling the δ-ferrite content at the austenite-martensite interface of the transition zone. The dotted line in the figure is the austenite-martensite interface line (A-M line) as determined by the authors on the basis of measurements of actual weld metal. The relationship between the δ-ferrite content on this A-M line and the coarse austenite grain ratio is shown in **Fig. 10**. It can be seen that the formation of coarse grains is

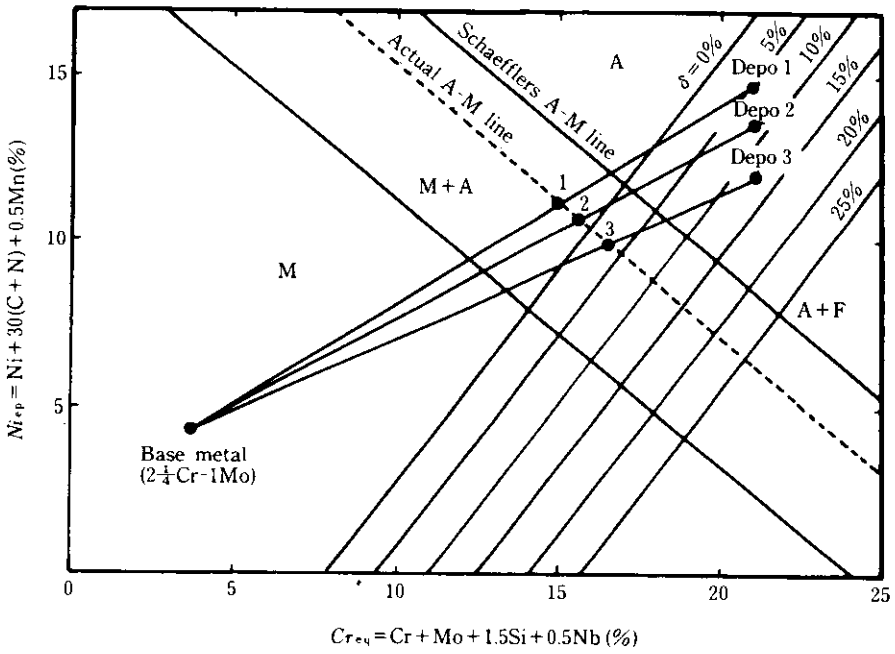

Fig. 9 Transition of microstructure from base metal to weld metal in the Delong and Schaeffler's diagram

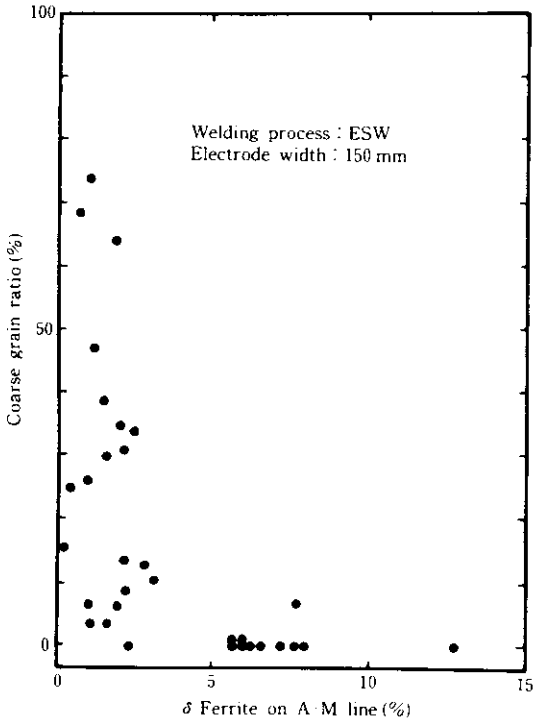

Fig. 10 Relation between the coarse grain ratio and the δ-ferrite contents along the A-M line in the Delong and Schaeffler's diagram

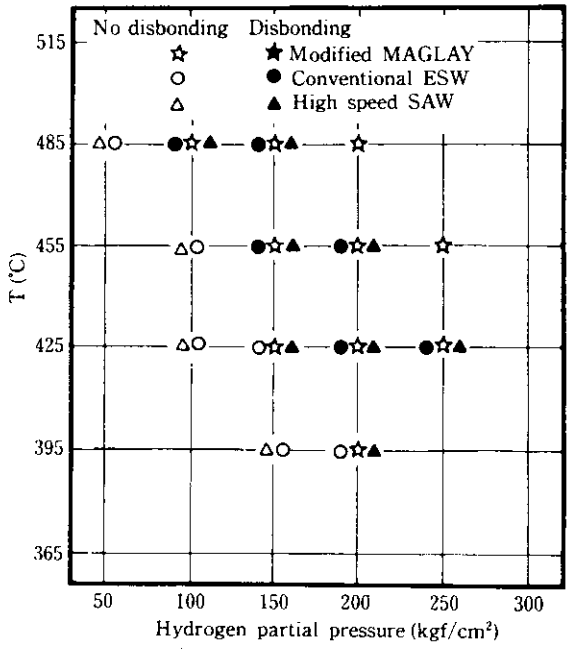

Fig. 11 Demonstration of the high resistivity against disbonding of the newly developed weld metal controlled silicon and δ-ferrite content

almost completely prevented when the δ-ferrite content on the A-M line is 5% or more.

Figure 11 is a diagram of hydrogen partial pressure and temperature, based on experimental results, showing the susceptibility of overlay weld metal to disbonding, in welds produced by modified MAGLAY method (marked ☆) developed by Kawasaki Steel. This figure also shows the characteristics of overlay weld metals obtained by high-speed SAW (marked ○) and conventional ESW (marked △).[21] The white symbols in the figure indicate that no disbonding occurred; the black, that disbonding was observed. These results

demonstrate that the modified MAGLAY method which properly controls the Si and δ-ferrite contents ensures the production of weld metal excellent in disbonding resistance.

5 Conclusions

Because of their excellent high-temperature mechanical properties and resistance to hydrogen degradation, Cr-Mo steels have been widely utilized as materials for equipment in the chemical industry, where operation in high-temperature and high-pressure hydrogen atmospheres is required. In the oil-refining industry, for example, equipment recently has tended to be constructed on a large scale with heavy sectioned steel plates or forgings and to be operated at higher temperatures and higher pressures in order to improve efficiency and cope with changes in the oil situation and the structure of demand. At present, the MPC (Metal Properties Council) of the U.S. plans to conduct research on the improvement of conventional $2\frac{1}{4}$Cr-1Mo steels in order to cope with these economic trends. An examination is being carried on into the utilization of elements of strong carbide formers, mentioned above, as part of this research. However, the increase in strength by addition of alloying elements usually tends to decrease toughness and SR cracking susceptibility. Therefore, it is necessary to evaluate characteristics of materials after a thorough examination of effects on these other properties.

At present, it is difficult to say that everything is clarified in terms of mechanism and phenomenon itself about the deterioration of steel that happens in its exceptionally long period of uses. For example, it has recently been found that the hydrogen attack resistance and SR sensitivity of $2\frac{1}{4}$Cr-1Mo steels can be substantially improved by reducing the S content to very low levels ($S < 0.002$ wt%).[22~24] To evaluate the reliability of materials under severe service conditions, it would be necessary to conduct studies more elaborate than heretofore so as to clarify the relationship between metallurgical factors and the deterioration in the mechanical properties that occurs during the service of materials.

References

1) T. Imanaka and J. Shimomura: "Temper Embrittlement and Hydrogen Attack on $2\frac{1}{4}$Cr-1Mo Steels in High Pressure and High Temperature Hydrogen Atmospheres," *Proc. of 15th Int. Conf. on Pressure Vessel Technology, Vol. II, Materials and Manufacturing*, (1985), 617-624
2) T. Imanaka: "Effect of Impurities on Hydroten Attack of $2\frac{1}{4}$Cr-1Mo Steels' *Preprint of Fall Meeting of the Japan Institute of Metals*, (1982), p. 245
3) T. Kotoyori: "Report on Burst of Desulphurizing Reactor of Heavy Oil in Kashima Petroleum Refinery", Saigai Kagaku Kenkyusho, January (1983)
4) "Steels for Hydrogen Services at Elevated Temperatures and Pressures in Petroleum Refineries and Petrochemical Plants," No. 941, 2nd ed., API, June (1977)
5) T. Imanaka: "Effect of Cr Content on Hydrogen Attack of Cr-Mo Steels", *Preprint of Fall Meeting of the Japan Institute of Metals*, (1984), p. 469
6) F. K. Naumann: "Der Einfluß von Legierungszusätzen auf die Beständigkeit von Stahl gegen Wasserstoff unter hohem Druck", *Stahl und Eisen*, **58**(1985)44, 1239-1250
7) T. Imanaka and S. Sato: "Effect of Vanadium on Hydrogen Attack Susceptibility and High Temperature Mechanical Properties of Cr-Mo Steels", to be published in *Tetsu-to-Haganė*
8) T. Imanaka: "On the Incubation Period for Hydrogen Attack of $2\frac{1}{4}$Cr-1Mo Steels", *Preprint of Fall Meeting of the Japan Institute of Metals*, (1983), p. 390
9) J. Pilling and N. Ridley: "Tempering of 2.25Pct Cr-1Pct Mo Low Carbon Steels," *Met. Trans. A*, **13A**(1982), 557
10) K. Yasuda, S. Nakano, T. Imanaka and N. Nishiyama: 'On disbonding of stainless steel weld overlay on vessel steels', *Symposium on disbonding in 89th committee of welding and metallurgy*, August (1982)
11) J. Tsuboi, T. Imanaka, S. Nakano, and K. Yasuda: "Development of Austenitic Stainless Steel Overlay Having an Excellent Resistivity against Disbonding", *Tetsu-to-Haganė*, **70**(1984),S669
12) M. Nakano, K. Yasuda, T. Imanaka and N. Nishiyama: "Weld Metal Composition Effective to Prevent Overlay Weld Cladding from Hydrogen Induced Disbonding," Kawasaki Steel Research Report, Presented at The Welding Institute Meeting, TWI, June (1983)
13) T. Imanaka, S. Nakano, and K. Yasuda: "Initial Phenomenon of Disbonding at Stainless Steel Overlay Weldments", *Tetsu-to-Haganė*, **69**(1983), S1371
14) "Handbook of High-Temperature Materials", No. 2 Properties Index., ed. by B. V. Samsonov, (1964), [Plenum Press]
15) F. D. Richardson: "The Thermodynamics of Metallurgical Carbides and of Carbon in Iron," *J. Iron and Steel Inst.*, **175**(1963) Sep., 33
16) R. C. Sharma, G. R. Purdy and J. S. Kirkaldy,: "Thermodynamics and Phase Equilibria for the Fe-C-Cr System in the Vicinity of the Euctectoid Temperature," *Met. Trans. A*, **10A**(1979) Aug., 1119
17) K. Kuo: "Carbides in Chromium, Molybdenum, and Tungsten Steels," *J. Iron and Steel Inst.*, **173**(1953) Apr., 363
18) W. Jellinghaus and H. Keller" "Das System Eisen-Chrom-Kohlenstoff und die Verteilung des Chroms Zwischen Ferrite und Sondercarbiden," *Arch Eisenhüttenwesen*, **43**(1972)4, 319
19) M. Small and E. Ryba: "Calculation of the Gibbs Energies of Formation of Cr_3C_2, Cr_7C_3 and $Cr_{23}C_6$," *Met Trans.*, **12A**(1981) Aug., 1389
20) G. H. Geiger and O. F. Angeles: "A Study of the Effects of High-Temperature, High Pressure Hydrogen on Low-Alloy Steels", *American Petroleum Institute Report No. 945*, API, Washington, D.C., 1975
21) T. Imanaka, T. Motoi, S. Nakano, and K. Yasuda: "Disbonding Characteristics of Stainless Steel Overlay by Improved MAGLEY Method", to be publidhed in *Tetsu-to-Haganė*
22) T. Imanaka and S. Sato: "Improvements in Elevated Temperature Embrittlement Properties of $2\frac{1}{4}$Cr-1Mo Steels" *Tetsu-to-Haganė*, 70(1984), S1481
23) T. Imanaka and S. Sato: "Improvements in Elevated Temperature Embrittlement Properties of $2\frac{1}{4}$Cr-1Mo Steels" *Preprint of High Pressure Institute of Japan* (1984), p. 5
24) T. Imanaka, S. Sato and J. Shimomura: "Improvements in the Susceptibility to Hydrogen Attack and Stress-Relief Cracking in $2\frac{1}{4}$Cr-1Mo Steels", to be presented at 1985 Midyear Meeting of American Petroleum Institute